Microstructural investigations of NiCrAlY+Y2O3 stabilized ZrO2 cermet coatings deposited by plasma transferred arc (PTA)

Camelia Demian, Alain Denoirjean, Lech Pawlowski, Paule Denoirjean, Rachida El Ouardi

Microstructural investigations of NiCrAlY + Y_2O_3 stabilized ZrO_2 cermet coatings deposited by plasma transferred arc (PTA)

Camélia Demian *, Alain Denoirjean, Lech Pawłowski, Paule Denoirjean, Rachida El Ouardi

SPCTS (UMR CNRS 7315), European Ceramic Center, University of Limoges, 87068 Limoges, France

Plasma transferred arc (PTA) deposition process was applied to develop high temperature protective cermet coatings, metallurgically bonded to the substrate. In this work, yttria-stabilized zirconia (YSZ) filler with two different particle sizes was added into NiCrAlY to develop cermet coatings. Microstructural characterizations using optical and scanning electron microscopes revealed that the addition of 20 vol.% of YSZ modified considerably the morphology of the coating. The formation of tetragonal zirconia, resulting from high temperatures and rapid solidification during surfacing process, was revealed by the X-ray diffraction of the NiCrAlY + 20YSZ composite. The microhardness filiation performed on the composites was influenced by the presence of the YSZ filler particles into the composite coatings.

1. Introduction

The protection of industrial tools against wear and corrosion is nowadays an important issue based on economic reasons. Ni based alloys are commonly used for surfacing industrial tools, e.g. hot forging dies [1], molds for the glass industry [2], etc. These alloys have outstanding mechanical properties especially at elevated temperatures from 400 to 800 °C, such as wear abrasion and corrosion resistances, as well as high stability of these properties. MCrAlY alloys are frequently used as functional top coating or for a bond coating and are particularly useful in protecting surfaces against high temperature degradation [3]. Furthermore, they can increase the durability and service life of substrates [4]. Due to their extensive applications in components protection of gas turbines and aero engines [5], many studies have been developed over the last decade, reporting on microstructural characterization or mechanical behavior testing [6] of such coatings.

A new area of such coating applications may be developed by adding filler particles to MCrAlY base matrix in order to form composite coatings. Thermally sprayed MCrAlY composite coatings with improved functional properties by the addition of reinforcements such as CeO_2 [6], Al_2O_3 [7], ceria/yttria stabilized zirconia (CSZ) (ZrO_2-25CeO_2-2.5Y_2O_3) [8], or yttria-stabilized zirconia (YSZ) (ZrO_2-8Y_2O_3) [9–11], are well known for their remarkable mechanical properties, corrosion resistance and thermal stability. However, the poor bonding between the splats of the metal oxide reinforcement (fillers) and the matrix, the formation of cracks or the porosity represent typical drawbacks of thermally sprayed coatings. Some post-spray treatments such as annealing [12] or laser remelting [13] may be useful in order to avoid or reduce these defects and to improve the coating – substrate bonding strength, or to induce a metallurgical bonding with the substrate.

Some of the drawbacks encountered in coatings developed by thermal spray processes can be eliminated by using surfacing techniques, such as laser cladding or plasma transferred arc (PTA). MCrAlY alloy and composite coatings were developed in particular by laser cladding process [14–18]. The method can be considered as an alternative to thermal spraying for high temperature protective coatings. Similar to laser cladding, PTA deposition process is a widely used process to develop Ni based composites [19,20] on different substrates. Influence of filler particles such as Cr_3C_2 [21,22], TiC–NiMo [23] or Mo [24,25] on the microstructure and properties of Ni based composites deposited by plasma transferred arc were also studied [26]. Finally, the improved mechanical behavior and refined microstructure were reported in the metal matrix composite (MMC) coatings obtained by PTA using 0.8 wt.% nano-Al_2O_3 particles filler in a nickel-based alloy matrix [27].

This paper focuses on the investigation of metal matrix composite (MMC) coatings deposited by PTA process. The composites were prepared using mechanical mixtures of YSZ (ZrO_2-13 wt.% Y_2O_3) having different volume concentrations which were incorporated in the NiCrAlY matrix. The morphology and the structure of the composite

* Corresponding author.
E-mail address: camelia.demian@unilim.fr (C. Demian).

coatings were analyzed by microscopic observations, energy dispersive spectroscopy and X-ray diffraction. Mechanical properties of the MMC coatings were evaluated by microhardness filiation.

2. Experimental conditions

2.1. MMC coatings elaboration

Substrate used for surfacing is medium carbon steel type AISI 1035 of 25 mm thickness (chemical composition: 0.35–0.39 wt.% C, ≤0.40 wt.% Si, 0.50–0.80 wt.% Mn, 0.015–0.035 wt.% S, ≤0.63 wt.% Cr + Ni + Mo and Fe balance). NiCrAlY powder used as matrix is a gas atomized powder (Fig. 1a). It is a commercial H.C. Starck powder AMPERIT 413.6 provided by Flame Spray Technologies BV, Netherlands with chemical composition of 22 wt.% Cr, 11 wt.% Al and 0.9 wt.% Y, and grain size distribution of 45–125 μm. ZrO_2-13 wt.% Y_2O_3 powders with grain size distributions of 22–45 μm (Fig. 1b) and 5–22 μm, provided by Medicoat (France) was used as filler. Three MMC powders were prepared by mechanical mixing of the two powders using: (i) YSZ with the granulation distribution of 22–45 μm (10 and 30 vol.% in the mixture); and (ii) YSZ with the granulation distribution of 5–22 μm (20 vol.% in the mixture) with NiCrAlY metal matrix powder. ZrO_2-13 wt.% Y_2O_3 was added to NiCrAlY matrix in order to lower the thermal conductivity of coatings. The variation in Y_2O_3 concentration results in stabilization of zirconia in different crystal phases.

The mixtures were mechanically blended and dried at a temperature of about 120 °C for 24 h. The substrate surface was prepared by grinding and preheating in an open air furnace at a temperature of about 365 °C for NiCrAlY + 10YSZ coating and 400 °C for NiCrAlY + 20YSZ and NiCrAlY + 30YSZ coatings in order to facilitate the metallic pool formation. The PTA surfacing was performed using numerical control equipment developed by DURUM S.A. (BARRAT Group), France. During the surfacing process, the temperature measurements of the melted pool were carried out using a FLIR SC600 infrared camera having a sensibility in the range of the wavelengths λ = 8 to 14 μm. The temperature measurements were performed at a distance of about 1.5 m from the sample surface. Emissivity of the metallic pool of $\varepsilon = 0.25$ was supposed.

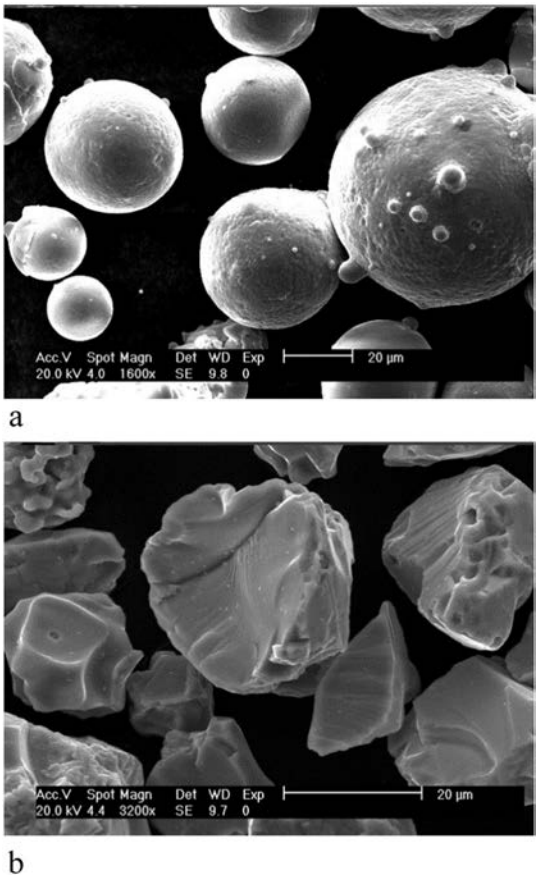

Fig. 1. SEM micrographs (secondary electrons) of the powders used for coatings deposition: a) NiCrAlY metal matrix powder; b) YSZ filler powder with grain size distribution of 22–45 μm.

The composite coatings were deposited in a single layer. The PTA surfacing variable parameters such as transferred arc current, voltage and surfacing real speed as well as the constant parameter during surfacing such as flow powder were reduced into one parameter which represents the principal factors of deposition Q (J·s/mm·g) calculated using Eq. (1):

$$Q = \frac{P}{v \cdot d} \tag{1}$$

where: P represents the electrical power of transferred arc (W); v represents the surfacing scan speed (mm/s) and d represents the powder feed rate (g/s).

The operational parameters used for MMC coatings processing are collected in Table 1. After the PTA processing the specimens were cooled down to the room temperature. Subsequently, they were subjected to a heat treatment at 500 °C for 2 h and left into the furnace to cool down to room temperature in order to reduce the residual stresses formed during the surfacing process.

2.2. Characterization methods

The composite coatings were characterized by examination of the morphology of coating – substrate system, in terms of macroscopic aspect, metallurgical bonding, and diffusion process between the chemical elements of the substrate and coating during surfacing. Dilution, as the amount of the base material participating on the coating, was determined by image analysis using ImageJ software on the microscopic images on single layer deposits. The samples were analyzed using Philips XL 30 scanning electron microscope (SEM) equipped with energy dispersive X-ray spectroscopy (EDS) analyzer. The samples were initially metallographically prepared following conventional procedure. The microstructure of the MMC coatings was revealed by electrochemical etching using chloric (HCl) and acetic (CH_3COOH) acids. The X-ray diffraction analysis was performed using a Bruker D8 ADVANCE equipment with a "lynx eye detector" and the monochromatic radiation of Cu-Kα1 with the wavelength of λ = 1.54060 nm. The acquisitions were made between angles $2\theta = 20°$ and 90°. The evaluation of mechanical properties using Vickers micro-hardness test was performed on the metallographic sections of the coatings using a Buehler MicroMet 6040 Vickers tester with a load of 300 g and a dwell time of 15 s.

3. Results and discussions

3.1. MMC coatings morphology

Fig. 2 presents the microstructures of NiCrAlY + 10YSZ, NiCrAlY + 20YSZ and NiCrAlY + 30YSZ coatings and their interfaces with the substrate. NiCrAlY + 20YSZ coating (Fig. 2c) has a similar aspect at its interface with substrate as the NiCrAlY + 10YSZ one (Fig. 2a). The island including oxides in the vicinity of interface with the substrate can be observed in the higher magnification image for the NiCrAlY + 20YSZ coating (Fig. 2c). The composite coatings including 10 and 20 vol.% of YSZ had a dilution of about 25%. Such dilution indicates a good bonding to the substrate. Smaller dilution and, consequently, poor bonding to the substrate can be observed in the case of NiCrAlY + 30YSZ coating. During the surfacing process an oxide layer including metallic particles was formed at the

Table 1
PTA experimental conditions.

Coating description	Parameter Q (J·s/mm·g)	Current of transferred arc (W)	Plasma gas flow rate Ar (L/min)	Shielding gas flow rate Ar + H_2 (L/min)	Oscillation speed (mm/s)	Powder carrier gas flow rate (L/min)	Torch to substrate distance (mm)
NiCrAlY + 10YSZ	4884	162	1.4	14	3.9	3.5	8
NiCrAlY + 30YSZ	4972	153			3.9		
NiCrAlY + 20YSZ	4001	160			4.9		

interface with substrate. Some fine cracks can also be observed in the coatings in the vicinity of the substrate. Due to the agglomeration of YSZ filler particles during the surfacing process, oxide islands were observed in all MMC coatings. The aspect of these islands is similar to the oxide layer at the interface with substrate, as it particularly easy to observe in NiCrAlY + 30YSZ coating (Fig. 2b). In general, a non-wetting behavior can be attributed to the nature of contact between the YSZ ceramic and NiCrAlY metallic matrix [28]. During the PTA process deposition, an amount of the YSZ particles were agglomerated to form the oxide islands or to the interface with substrate, while another amount was dispersed into the matrix. After the coating deposition, more oxide islands were formed into the coatings with larger particle size of YSZ due to the larger contact area with the metallic matrix. This is also due to the larger amount of YSZ filler in the case of NiCrAlY + 30YSZ coating. The reason of using composite mixtures containing two sizes of YSZ particles was to test which size of filler particle is suitable to obtain homogeneous coatings using PTA process. The formation of the islands is correlated to the process parameters and especially with Q-parameter. The parameter was required to be high in order to obtain the coatings having large size of YSZ particles. Inversely, this parameter was smaller to obtain the coating with small size filler particles. Using a lower oscillation speed correlated with high current of transferred arc, metallurgical bonding was realized between the NiCrAlY + 10YSZ coating and substrate. In the case of NiCrAlY + 30YSZ, keeping constant the oscillation speed but decreasing the current of transferred arc, oxide islands were formed at the interface with substrate. Then, the oscillation speed and current of transferred arc were increased for the deposition of NiCrAlY + 20YSZ to assure high energy dispersion on the local contact between plasma of transferred arc and substrate. Moreover, low oscillation speed contributes in increasing of Q-parameter (see Eq. (1)).

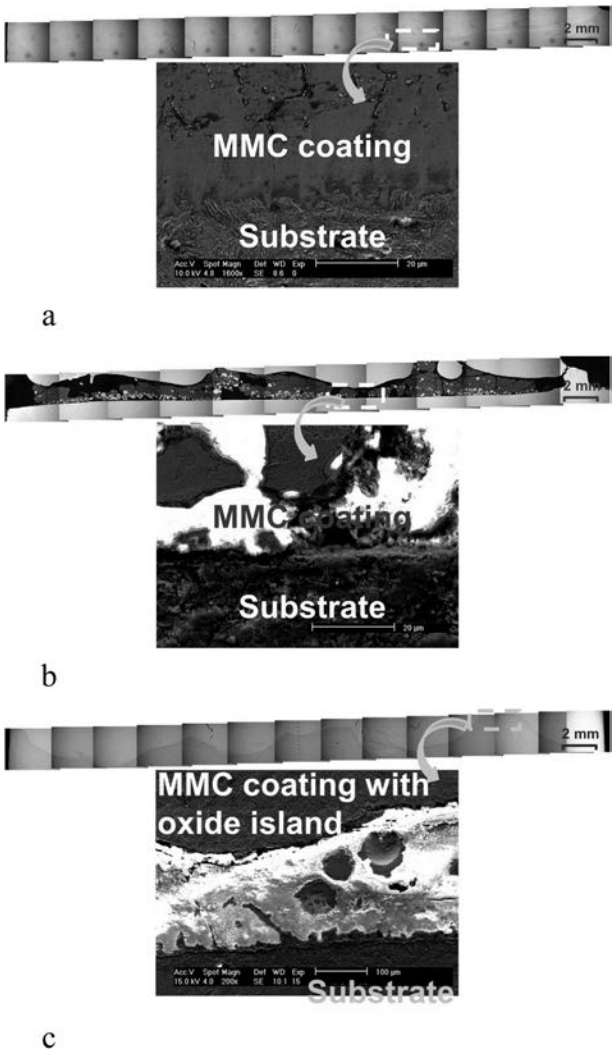

Fig. 2. MMC coating-substrate interface (not etched and etched samples for macroscopic and microscopic aspect respectively): a) NiCrAlY + 10YSZ; b) NiCrAlY + 30YSZ (filler size of 22–45 μm); c) NiCrAlY + 20YSZ (filler size of 5–22 μm).

A dendritic microstructure was observed in all three composite coatings (see Figs. 3–5). The matrix has a modified γ-Ni phase/β-NiAl phase solidification microstructure, typical of the laser cladded MCrAlY alloys as shown elsewhere [15]. EDS microanalyses of the MMC coatings are shown in Figs. 3b, 4b and 5b and revealed a Ni matrix with Cr and Fe. The presence of iron into the matrix coatings can be explained by the element diffusion from the substrate into the coatings during the surfacing process. The additional EDS microanalysis made at the interface of coating and substrate for NiCrAlY + 10YSZ coating confirmed the Fe diffusion. The intermetallic (Ni,Al) phase was observed in the interdendritic zones for all the processed coatings. Moreover, the initial filler particles of YSZ were also detected in the interdendritic zones. This can be explained by the contact between a solid ceramic particle as YSZ and the metallic pool of NiCrAlY at high temperatures attained during processing. The NiCrAlY + 10YSZ coating has a small porosity in the vicinity of the YSZ particles (Fig. 3a). Contrary, the NiCrAlY + 30YSZ and NiCrAlY + 20YSZ had no such porosity (Figs. 4a and 5a). The presence of the porosity into the composite coating (including matrix) with a lower amount of YSZ filler particles (NiCrAlY + 10YSZ) comparing to the NiCrAlY + 30YSZ can be due to the lower value of Q-parameter. This was obtained by using a higher current of the transferred arc at the elaboration process (Table 1) correlated with a lower substrate temperature. The preheating temperature of the substrate (365 °C) was also kept constant during the processing. Finally, it was impossible to obtain dense coating. The lower particle sizes deposited at constant pressure of carrier gas improved the microstructure of the coating containing 20% of YSZ. The dispersion of the small size of YSZ particles was better in such coating.

EDS microanalysis on an oxide island formed into the NiCrAlY + 20YSZ coating is shown in Fig. 6 and reveals a few phases. Solidified matrix particles inserted into the oxide island were observed. The EDS microanalysis reveals the presence of Ni solid solution with

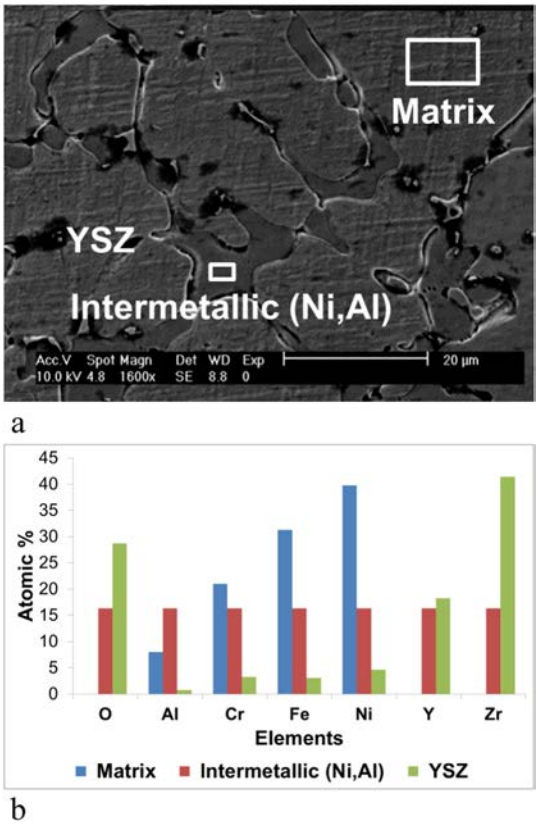

Fig. 3. SEM microstructure (a) and EDS elemental composition microanalyses (b) of NiCrAlY + 10YSZ (etched sample).

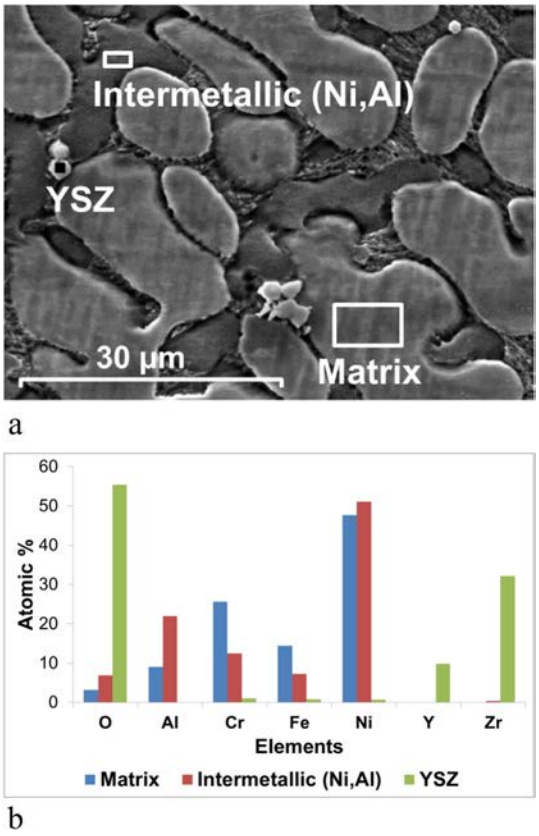

Fig. 4. SEM microstructure (a) and composition microanalyses (b) of NiCrAlY + 30YSZ (etched sample).

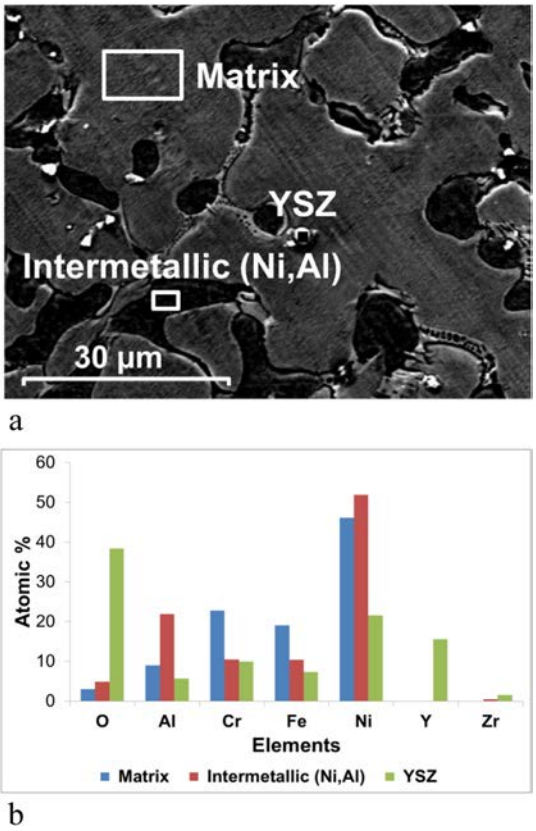

Fig. 5. SEM microstructure (a) and composition microanalyses (b) of NiCrAlY + 20YSZ (etched sample).

intergranular Cr and (Zr,Y,O) based phases and an Al based phase. On the contrary, the oxide island includes (Zr,Y,O) intragranular phase and (Al,O) intergranular phase.

The structures of the three composite coatings are similar. The X-ray diffraction diagram of the NiCrAlY + 20YSZ was investigated and compared to those of initial powders (see Fig. 7). It confirmed the presence of the precipitated phases.

The metal matrix powder is composed of several phases: Cr, Al and β (Ni,Al) in Ni solid solution and a secondary (Ni,Y) compound. The YSZ filler powder is composed of two phases: a main ZrO_2 cubic phase and a secondary phase of monoclinic ZrO_2. The X-ray diffraction diagram of the composite coating analyzed in longitudinal section revealed few low intensity peaks of Cr and β (Ni,Al) phases and does not show any ZrO_2 phase. This indicates the preferential growth in single direction of the dendrites oriented perpendicular to the substrate. The X-ray diffraction of the composite coating was analyzed on the transversal section and indicated similar metallic phases in Ni solid solution and two ZrO_2 phases: cubic and tetragonal. The monoclinic zirconia was not detected. The rapid heating and cooling during the surfacing process could have led to the conversion of the cubic phase into tetragonal phase. Similar phase transformation was reported in the case of composite NiCrBSi + 60 vol.% YSZ coatings elaborated by laser cladding [29]. The analysis of phase diagram of zirconia – yttria system indicates that at the cooling from the melting point, zirconia has a first structural transformation from cubic to tetragonal at about 2340 °C and the second one, from tetragonal to monoclinic at about 1170 °C [30]. Thus, the tetragonal zirconia phase revealed by the X-ray diffraction of the composite coating could have resulted from the structural transformation of zirconia from monoclinic to tetragonal at about 1200 °C. The structural transformation of zirconia was possible because of high temperatures attained during the PTA coating deposition. The temperature of the metal pool was measured to be in the range from 1800 to about

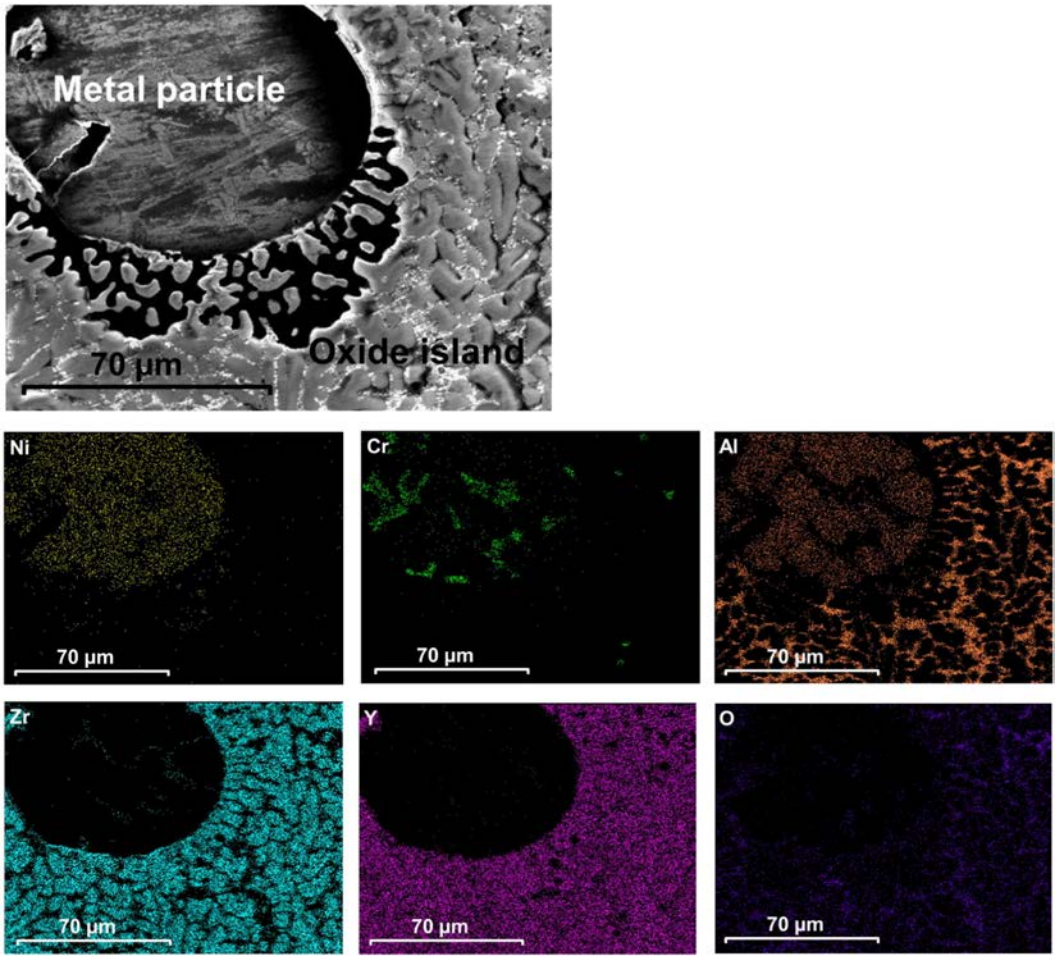

Fig. 6. SEM microstructure and EDS elemental maps microanalyses of an oxide island (NiCrAlY + 20YSZ coating – etched sample).

2400 °C. The solidification process of the metal pool is quite longer in time (about ms) for the PTA process comparing to laser cladding.

3.2. MMC coatings mechanical properties

Vickers microhardness filiation was realized. Fig. 8 shows the $HV_{0.3}$ values for the MMC coatings through the heat affected zone (HAZ) and down to the substrate.

Three different levels of hardness such as lowest $HV_{0.3}$ for the substrate, intermediate $HV_{0.3}$ for the HAZ and highest $HV_{0.3}$ for the MMC coating can be observed in all tested cases. The oxide islands detected in the MMC coatings reached the values of about 1500 $HV_{0.3}$ in all three cases. The satisfactory average microhardness is 493 ± 38, 482 ± 40 and 309 ± 33 $HV_{0.3}$ for NiCrAlY + 10YSZ, NiCrAlY + 30YSZ and NiCrAlY + 20YSZ coatings respectively. For the coatings with metallurgical bonding (NiCrAlY + 10YSZ, NiCrAlY + 20YSZ) lower values of microhardness of about 250 $HV_{0.3}$ can be observed in the vicinity of the interface with substrate. This can be explained by diffusion of Fe into the coating in proportion of about 20% for NiCrAlY + 20YSZ (Fig. 5b) and 30% for NiCrAlY + 10YSZ (Fig. 3b). The higher average hardness of the

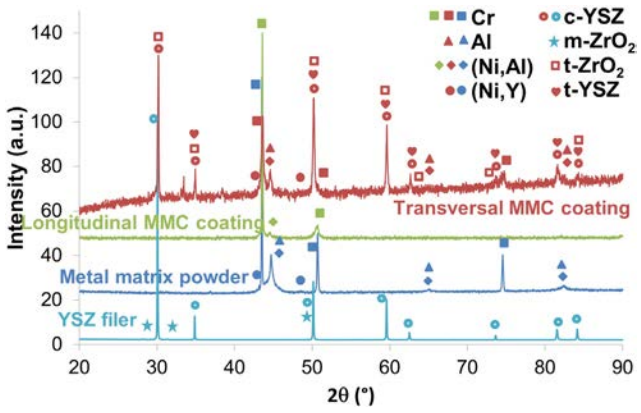

Fig. 7. X-ray diffraction diagrams of NiCrAlY + 20YSZ coating; YSZ filler and NiCrAlY matrix initial powders.

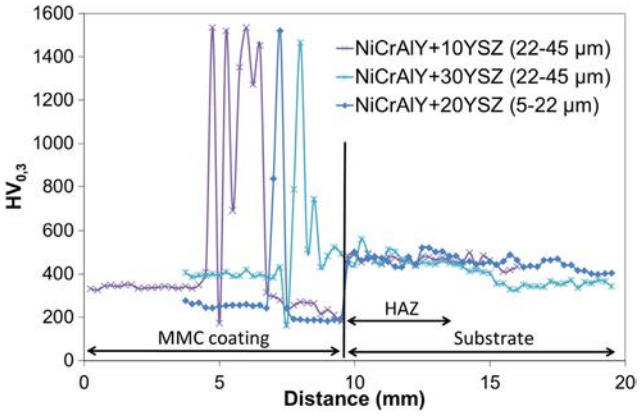

Fig. 8. Vickers micro-hardness filiation of the MMC coatings (HAZ represents the heat affected zone).

NiCrAlY + 10YSZ and NiCrAlY + 30YSZ coatings is due to the oxide islands (higher hardness points in the Fig. 8) presented in the coatings in a higher proportion comparing to the NiCrAlY + 20YSZ coating. However, lower average microhardness can be noted in the case of NiCrAlY + 20YSZ. This is possible due to the smaller particle size of YSZ filler well distributed into the NiCrAlY matrix during the PTA processing. Absence of microstructural defects such as oxide islands was detected in the case of NiCrAlY + 20YSZ coating. The good metallurgical bonding to the substrate correlated with high energies induced during surfacing by higher scan speed (see Table 1) conducted to lower down the average microhardness.

4. Conclusions

The composite coatings of NiCrAlY with an addition of 10, 20 and 30 vol.% YSZ were deposited on the medium carbon steel using plasma transferred arc process. Using high currents of transferred arc, good metallurgical bonding between the coating and substrate can be obtained in the case of NiCrAlY + 10YSZ and NiCrAlY + 20YSZ coatings.

The microstructure analysis revealed some porosity in the vicinity of the larger YSZ particles (22–45 μm) for the NiCrAlY + 10YSZ coating. NiCrAlY + 30YSZ coating (larger YSZ particles: 22–45 μm) did not reveal such porosity but the metallurgical bonding was not realized. NiCrAlY + 20YSZ coating with small filler grain size (5–22 μm) did not reveal porosity. In spite of the not wetting behavior between the liquid matrix and YSZ ceramic, the smallest YSZ particles could have been incorporated into the NiCrAlY matrix due the limited contact area.

Some oxide islands detected in all composite coatings formed during the surfacing process might have resulted from the agglomeration of the YSZ particles. The X-ray diffraction enabled the detection of the tetragonal zirconia. Composite coatings with larger particle sizes presented high average Vickers microhardness ($HV_{0.3}$): 493 ± 38 for NiCrAlY + 10YSZ and 482 ± 40 for NiCrAlY + 30YSZ due to the presence of the oxide islands. NiCrAlY + 20YSZ coating presented an average Vickers microhardness ($HV_{0.3}$) of 309 ± 33 explained by the reduced number of oxide islands.

Finally, it was found out that cermet coatings including small particles of YSZ filler in a concentration of 20 vol.% into a NiCrAlY matrix was the optimal choice among all tested in the presented conditions. This is due to the better incorporation of YSZ small particles into the metal matrix, good metallurgical bonding to the substrate, and the absence of microstructural defects in the coating morphology but lower microhardness. Regarding mechanical properties, the best option might be NiCrAlY + 10YSZ and NiCrAlY + 30YSZ to further realize composite coatings using PTA process.

Acknowledgements

The authors express their grateful acknowledgements to the Limousin Region (grant number: SAFIR 11-5148) and the Limousin FEDER (grant number: 36246) for financial support within the FUI project: ROOF2 (grant number: Bpi F1201011C).

References

[1] H. Kashani, A. Amadeh, H.M. Ghasemi, Room and high temperature wear behaviors of nickel and cobalt base weld overlay coatings on hot forging dies, Wear 262 (2007) 800–806.
[2] F. Fernandes, B. Lopes, A. Cavaleiro, A. Ramalho, A. Loureiro, Effect of arc current on microstructure and wear characteristics of a Ni-based coating deposited by PTA on gray cast iron, Surf. Coat. Technol. 205 (2011) 4094–4106.
[3] S.B. Mishra, K. Chandra, S. Prakash, Erosion–corrosion performance of NiCrAlY coating produced by plasma spray process in a coal-fired thermal power plant, Surf. Coat. Technol. 216 (2013) 23–34.
[4] X. Ren, F. Wang, High-temperature oxidation and hot-corrosion behavior of a sputtered NiCrAlY coating with and without aluminizing, Surf. Coat. Technol. 201 (2006) 30–37.
[5] A.G. Evans, D.R. Mumm, J.W. Hutchinson, G.H. Meier, F.S. Pettit, Mechanisms controlling the durability of thermal barrier coatings, Prog. Mater. Sci. 46 (2001) 505–553.
[6] X. Sun, S. Chen, Y. Wang, Z. Pan, L. Wang, Mechanical properties and thermal shock resistance of HVOF sprayed NiCrAlY coatings without and with nano ceria, J. Therm. Spray Technol. 21 (5) (2012) 818–824.
[7] L. Zhou, W. Zhou, F. Luo, J. Su, D. Zhu, Y. Dong, Microwave dielectric properties of low power plasma sprayed NiCrAlY/Al_2O_3 composite coatings, Surf. Coat. Technol. 210 (2012) 122–126.
[8] J.H. Lee, D.B. Lee, Hot corrosion of NiCrAlY/(ZrO_2–CeO_2–Y_2O_3) composite coatings in NaCl–Na_2SO_4 molten salt, Mater. Sci. Forum 658 (2010) 228–231.
[9] C. Zhu, Y.G. Wang, L.N. An, A. Javed, P. Xiao, G.Y. Liang, Microstructure and oxidation behavior of conventional and pseudo graded NiCrAlY/YSZ thermal barrier coatings produced by supersonic air plasma spraying process, Surf. Coat. Technol. (2015), http://dx.doi.org/10.1016/j.surfcoat.2015.04.014.
[10] D.B. Lee, C. Lee, High-temperature oxidation of NiCrAlY/(ZrO_2–Y_2O_3 and ZrO_2–CeO_2–Y_2O_3) composite coatings, Surf. Coat. Technol. 193 (2005) 239–242.
[11] A.M. Khoddami, A. Sabour, S.M.M. Hadavi, Microstructure formation in thermally-sprayed duplex and functionally graded NiCrAlY/Yttria-stabilized zirconia coatings, Surf. Coat. Technol. 201 (2007) 6019–6024.
[12] G. Zhang, A.F. Kanta, W.Y. Li, H. Liao, C. Coddet, Characterizations of AMT-200 HVOF NiCrAlY coatings, Mater. Des. 30 (2009) 622–627.
[13] B.S. Sidhu, D. Puri, S. Prakash, Characterisations of plasma sprayed and laser remelted NiCrAlY bond coats and Ni3Al coatings on boiler tube steels, Mater. Sci. Eng. A368 (2004) 149–158.
[14] R. Vilar, E.C. Santos, P.N. Ferreira, N. Franco, R.C. da Silva, Structure of NiCrAlY coatings deposited on single-crystal alloy turbine blade material by laser cladding, Acta Mater. 57 (2009) 5292–5302.
[15] C. Bezençon, A. Schnell, W. Kurz, Epitaxial deposition of MCrAlY coatings on a Ni-base superalloy by laser cladding, Scr. Mater. 49 (2003) 705–709.
[16] J.C. Pereira, J.C. Zambrano, M.J. Tobar, A. Yañez, V. Amigó, High temperature oxidation behavior of laser cladding MCrAlY coatings on austenitic stainless steel, Surf. Coat. Technol. 270 (2015) 243–248.
[17] H. Wang, D. Zuo, X. Li, K. Chen, M. Huang, Effects of CeO_2 nanoparticles on microstructure and properties of laser cladded NiCoCrAlY coatings, J. Rare Earths 28 (2) (2010) 246–250.
[18] K. Partes, C. Giolli, F. Borgioli, U. Bardi, T. Seefeld, F. Vollertsen, High temperature behaviour of NiCrAlY coatings made by laser cladding, Surf. Coat. Technol. 202 (2008) 2208–2213.
[19] C. Sudha, P. Shankar, R.V. Subba Rao, R. Thirumurugesan, M. Vijayalakshmi, B. Raj, Microchemical and microstructural studies in a PTA weld overlay of Ni–Cr–Si–B alloy on AISI 304L stainless steel, Surf. Coat. Technol. 202 (2008) 2103–2112.
[20] F. Fernandes, A. Cavaleiro, A. Loureiro, Oxidation behavior of Ni-based coatings deposited by PTA on gray cast iron, Surf. Coat. Technol. 207 (2012) 196–203.
[21] Z. Huang, Q. Hou, P. Wang, Microstructure and properties of Cr_3C_2-modified nickel-based alloy coating deposited by plasma transferred arc process, Surf. Coat. Technol. 202 (2008) 2993–2999.
[22] A. Zikin, I. Hussainova, C. Katsich, E. Badisch, C. Tomastik, Advanced chromium carbide-based hardfacings, Surf. Coat. Technol. 206 (2012) 4270–4278.
[23] A. Zikin, E. Badisch, I. Hussainova, C. Tomastik, H. Danninger, Characterisation of TiC–NiMo reinforced Ni-based hardfacing, Surf. Coat. Technol. 236 (2013) 36–44.
[24] Q.Y. Hou, Z.Y. Huang, N. Shi, J.S. Gao, Effects of molybdenum on the microstructure and wear resistance of nickel-based hardfacing alloys investigated using Rietveld method, J. Mater. Process. Technol. 209 (2009) 2767–2772.
[25] Q.Y. Hou, Influence of molybdenum on the microstructure and properties of a FeCrBSi alloy coating deposited by plasma transferred arc hardfacing, Surf. Coat. Technol. 225 (2013) 11–20.
[26] L. Pawlowski, Dépôts Physiques, PPUR, Lausanne, Suisse, 2003.
[27] Q.Y. Hou, Z. Huang, J.T. Wang, Influence of nano-Al_2O_3 particles on the microstructure and wear resistance of the nickel-based alloy coating deposited by plasma transferred arc overlay welding, Surf. Coat. Technol. 205 (2011) 2806–2812.
[28] M.C. Munoz, S. Gallego, J.I. Beltran, J. Cerda, Adhesion at metal-ZrO_2 interfaces, Surf. Sci. Rep. 61 (2006) 303–344.
[29] Y.T. Pei, J.H. Ouyang, T.C. Lei, Laser cladding of ZrO_2–(Ni alloy) composite coating, Surf. Coat. Technol. 81 (1996) 131–135.
[30] H.G. Scott, Phase relationships in the zirconia-yttria system, J. Mater. Sci. 10 (1975) 1527–1535.